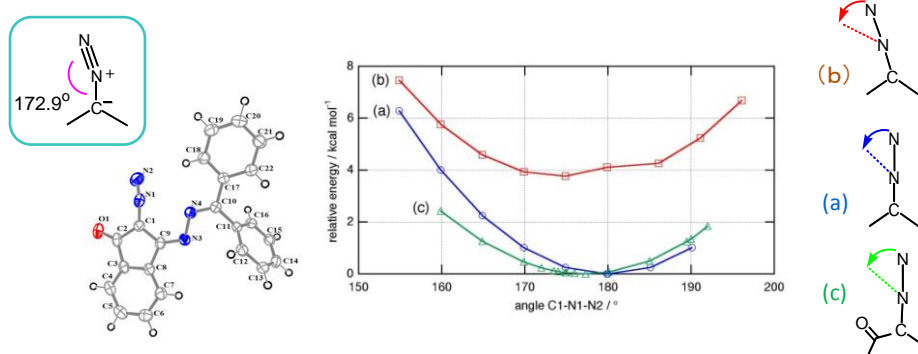


## Graphical Abstract



## Bent CNN bond of diazo compounds, $RR'(C=N^+=N^-)$

Motoko Akita,<sup>†</sup> Mai Takahashi,<sup>†</sup> Keiji, Kobayashi,<sup>†\*</sup> Naoto Hayashi, and Hideyuki, Tukada<sup>§</sup>

<sup>†</sup> *Graduate School of Science, Josai University, Sakado, Saitama 350-0295, Japan*

<sup>‡</sup> *Graduate School of Science and Engineering, University of Toyama, Gofuku, Toyama 930-8555, Japan*

<sup>§</sup> *International Graduate School of Arts and Science, Yokohama City University, Seto, Kanazawa-ku, Yokohama 236-0027, Japan*

### Abstract

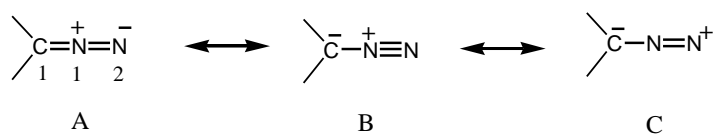
The reaction of ninhydrin with benzophenone hydrazone afforded 2-diazo-3-diphenylmethylenehydrazono-2-indanone **1** and 2-diazo-1,3-bis(diphenylmethylenehydrazono)indane **2**. X-ray crystal structure analyses of these products showed that the diazo functional group  $C=N^+=N^-$  of **1** is bent by  $172.9^\circ$ , while that of **2** has a linear geometry. The crystal structure data of diazo compounds have been retrieved from the Cambridge Structural Database (CSD), which hit 177 entries to indicate that the angle of  $172.9^\circ$  in **1** lies in one of the most bent structures. The CSD search also indicated that diazo compounds consisting of a distorted diazo carbon tend to bend the  $C=N^+=N^-$  bond. On the basis of DFT calculations (B3LYP/6-311++G(d,p)) of model compounds, it was revealed that the bending of the CNN bond is principally induced by steric factors and that the neighboring carbonyl group also plays a role in bending toward the carbonyl side owing to an electrostatic attractive interaction. The potential surface along the path of  $C=N^+=N^-$  bending in 2-diazopropane shows a significantly shallow profile with only 4 kcal/mol needed to bend the  $C=N^+=N^-$  bond from  $180^\circ$  to  $160^\circ$ . Thus, the bending of the diazo group in **1** is reasonable as it is provided with all of the factors for facile bending disclosed in this investigation.

### 1. Introduction

There has been much interest in diazoalkanes for many years [1], because of their usefulness as precursors to carbenes, which are intermediates in the photolysis and thermolysis of diazoalkanes, and more recently as a consequence of work on molecular

magnetism based on persistent triplet carbenes [2]. In contrast to the wealth of well-established reactions of diazo compounds, the structural aspect of these compounds has attracted much less attention after resolving their early issue, *i.e.*, which is the true configuration, the acyclic (diazirine) or open configuration [3].

A common understanding of the structure of the diazo functional group C1-N1-N2 is that it has a linear geometry, which is represented by a resonance hybrid between the canonical forms A, B, and C. The carbon atom C1 is essentially sp<sup>2</sup>-hybridized and both nitrogen atoms have sp hybridization: the three atoms C, N, and N should have a linear geometry [4]. These structural features are deduced from results of a number of X-ray crystallographic analyses, in which the C1-N1 and N1-N2 bond lengths have been mainly noted whereas the CNN angle has been little remarked on.



In the course of our study of the preparation of new  $\pi$ -expanded azine compounds using the reaction of carbonyl compounds with hydrazones, we have unexpectedly obtained the novel diazo compounds, 2-diazo-3-diphenylmethylenehydrazono-2-indanone (**1**) and 2-diazo-1,3-bis(diphenylmethylenehydrazono)indane (**2**). The structures of these products were determined by X-ray crystallographic analysis. The characteristic feature observed in **1**, that is, a bent bond of the diazo C1-N1-N2 group, prompted us to search the database of Cambridge Structural Database (CSD) for the structural outcome of diazo compounds. Herein, we report our findings regarding the bent structure of the diazo functional group, which has been overlooked to date.

## 2. Experimental

### 2.1. Materials and methods

A mixture of benzophenone hydrazone (0.98 g, 5.0 mmol) and ninhydrin (1.35 g, 7.6 mmol) in methanol (50 mL) was mixed with five drops of acetic acid at room temperature for 3 hr. The mixture was poured into water, and extracted with dichloromethane. The combined organic phases were washed with water and brine and dried over anhydrous MgSO<sub>4</sub>. The product mixture left after solvent removal was

chromatographed on a silica gel column using dichloromethane as an eluent. Azine **3** was eluted fast, and then compound **1** was eluted followed by compound **2**. Analytically pure **1** and **2** were isolated by further purification using gel permeation chromatography (GPC, JAIGEL 1H and 2).

**1**: Yield: 14%. M.p. 180-182 °C. <sup>1</sup>H NMR (400 MHz, CD<sub>3</sub>CN): δ 7.39-7.42 (2H, m), 7.44-7.53 (m, 6H), 7.56-7.58 (2H, m), 7.64-7.68 (m, 3H), 7.76-7.79 (m, 1H). Fab-MS (m/z): 350+1(62%), 306+1(31%), 153+1(100%). <sup>13</sup>C NMR (100.4 MHz, CDCl<sub>3</sub>): δ 122.5, 122.7, 127.6, 129.4, 129.2, 129.5, 130.4, 130.7, 131.3, 131.7, 133.8, 134.6, 135.9, 137.6, 138.0, 154.1, 165.9, 185.0 ppm. IR (KBr): 2095 (NN str.), 1688 (CO str.) cm<sup>-1</sup>.

**2**: Yield: 8%. M.p. 210-212 °C. <sup>1</sup>H NMR (400 MHz, CDCl<sub>3</sub>): δ 7.38-7.41 (4H, m), 7.42-7.51 (14H, m), 7.53-7.57 (6H, m). <sup>13</sup>C NMR (100.4 MHz, CDCl<sub>3</sub>): δ 120.1, 125.5, 126.4, 127.0, 127.4, 128.2, 128.5, 129.1, 132.8, 132.9, 134.7, 136.0, 153.5, 162.0 ppm. MS (m/z): 528+1 (16%), 306+1(29%), 288+1(14%), 153+1 (100%). IR (KBr): 2095 (NN str.) cm<sup>-1</sup>.

## 2.2. X-ray crystal structure analysis

An X-ray analysis of **1** and **2** was performed using single crystals recrystallized from acetonitrile. X-ray diffraction data were collected on a Rigaku RAXIS RAPID imaging plate area detector with graphite monochromated Mo-K $\alpha$  radiation ( $\lambda$ =0.71075 Å). Diffraction data were collected at -100 °C for both **1** and **2**. The crystal structures were solved by the direct method using SHELX97 for **1** and SIR92 for **2** and refined by the full-matrix least-squares method [5]. Non-hydrogen atoms were placed at calculated positions with C-H = 0.95 Å and refined using the riding model. All calculations were performed using the CrystalStructure 3.8.2 crystallographic software package [6,7]. Structural parameters are listed in Table 1.

Crystal data and other experimental details have been deposited at the Cambridge Crystallographic Data Centre (CCDC). **1**: CCDC885009. **2**: CCDC885010.

## 2.3. Database search

Database search was carried out using CSD (version 5.33 Nov. 2011) + 2updates [8] using the program ConQuest (ver.1.12) [9]. The diazo group (CNN) was defined as a structural fragment comprising of a nitrogen atom (N2) with one bond, a nitrogen

atom (N1) with two bonds, and a carbon atom (C1) with three bonds and linked in the C1-N1-N2 sequence of these three atoms. Thus, all canonical representations of the diazo functional group, regardless of A, B, C, and others, are included. Then, the CNN structure, in which the carbon atom (C1) is bonded to carbon or hydrogen atoms such as C-(CNN)-C and C-(CNN)-H, was generated, limiting the search to organic and noncoordinating compounds. The search gave 177 hits (144 crystal structures), which dropped to 150 (125 crystal structures) after the following filtering: (a) no crystallographic disorder and (b) an R-factor of less than 0.1.

## **2.4. DFT calculations**

Optimized structures were obtained by density functional theory (DFT) calculations, which were performed with the Gaussian 09 and 09W program suites [10]. The calculations employed the B3LYP exchange-correlation functional, which combines the hybrid exchange functional of Becke [11,12] with the gradient-correlation functional of Lee-Yang-Parr [13]. Basis sets with polarization functions and diffuse functions 6-311++G(d,p) were stored internally in the Gaussian 09 (09W) program packages. The X-ray geometries for **1** and **2** were used as a starting point for the calculations. All the optimized structures had no imaginary frequencies. Potential energy surfaces (PESs) along a C-N-N bending pathway were calculated with a fully relaxed scan method.

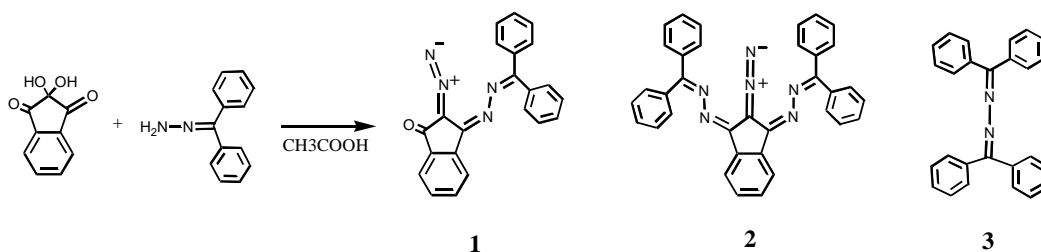
## **3. Results and discussion**

### **3.1. Formation of diazo compounds 1 and 2**

Ninhydrin is known as a highly electrophilic compound because of its activated ketone functional group at the 2-position [14]. It reacts with a variety of nucleophiles such as amines [15] as well as phenols, and methylene compounds activated by a neighboring carbonyl group. We have carried out the reaction of ninhydrin with benzophenone hydrazone in acetic acid and isolated monodiazo compound **1** in 14% yield along with tetraphenyl ketazine **3** in 8%. Compound **2** was isolated only in trace amount, being not sufficient to characterize by spectroscopic methods, whereas its structure could be determined on the basis of X-ray crystallographic analysis.

The reaction of ninhydrin with tosylhydrazine to afford 2-diazo-1,3-indandione has been known as the Bamford-Stevens reaction [16,17], while diazotization by hydrazone

has rarely been encountered. It seems likely that benzophenone hydrazone reacts first at the most electrophilic site of ninhydrin, followed by condensation with the carbonyl group at the 1- or 3-position to give highly congested bis- or tri-azine compounds, which would decompose to **1** and **2** to release steric hindrance via a process analogous to the Bamford-Stevens reaction [18].



[Scheme 1 Reaction of ninhydrin with benzophenone hydrazone]

### 3.2. X-ray crystal structure of **1** and **2**

On recrystallization from acetonitrile **1** crystallizes into a monoclinic lattice with  $P2_1/a$  symmetry. The crystal data and structure refinement of **1** are shown in Table 1. The ORTEP diagram is shown in Fig. 1, and displacement ellipsoids are drawn at a 50% probability level. Some selected geometric parameters are given in Table 2.

[Table 1 Crystal and experimental data of **1** and **2**]

[Table 2 Selected bond lengths (Å) and angles (°) for **1** and **2**]

The indan skeleton of **1** is planar including the three atoms O, N, and N attached to this ring. The N-N bond of the azine moiety =N-N= is directed toward the diazo group and adopts an *s-trans* conformation to bring about a close intramolecular contact of 2.804 Å between the N atoms of the diazo and azine groups. As a result, the azine unit C=N-N is also on the same plane of the indan unit, while the >C=N- moiety derived from benzophenone hydrazone is slightly distorted from this plane (C=N-N=C torsion angle: 167.69°). The molecules are stacked facing this molecular plane to form an infinite chain along the *a*-axis. Thus, face-to-face  $\pi$ ,  $\pi$ -interactions are realized between neighboring molecules along with face-to-edge  $\pi$ ,  $\pi$ -interactions using one of the phenyl rings of the N=C(Ph)<sub>2</sub> moiety, which has a conformation nearly perpendicular to the other phenyl ring.

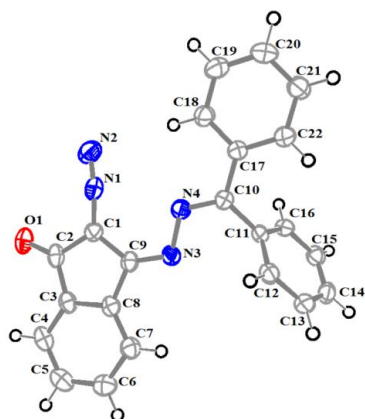


[**Fig. 1.** Molecular structure of **1** with ellipsoids drawn at 50 % probability level.]

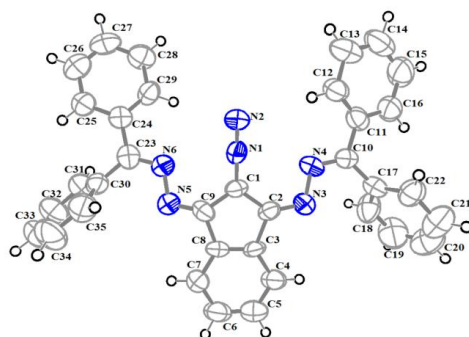


[**Fig. 2.** Molecular structure of **2** with ellipsoids drawn at 50 % probability level.]

The azide group plays no role in any intermolecular interaction but only participates in intramolecular N—N contact. The N=N and N=C distances of the diazo group are 1.128 and 1.319 Å, respectively. Contrary to the assumption based on atomic radius, the N=N bond is shorter than the N=C bond, indicating that the N---N bond has a more pronounced multibond character than the C---N bond. The most interesting feature in the molecular structure of **1** is the bent bond of the diazo functional group: the  $\text{C}=\text{N}^+=\text{N}^-$  bond is not in a linear geometry but is bent to  $172.9^\circ$  towards the carbonyl site approximately on the same plane made by the indanone framework (torsion angle of  $\text{O}=\text{C}-\text{C}=\text{N}$ ;  $0.37^\circ$ ).

The X-ray molecular structure of **2** was determined for a single crystal obtained by recrystallization from acetonitrile. The crystal data and structure refinement of **2** are shown in Table 3. The ORTEP diagram is shown in Fig. 2. The selected bond

lengths, bond angles and torsions are listed in Table 2. The C1-N1-N2 bond is close to a linear geometry (CNN angle:  $177.98^\circ$ ) in contrast to that of **1**. The two azine moieties as well as the diazo group are slightly twisted from the plane made by the indan skeleton (torsion angles of C=N-N=C:  $178.99$ ,  $177.76^\circ$ ), whereas the N1 atom is situated closely to two azine nitrogen atoms nearly on the same plane and subject to intermolecular N...N interactions with short N...N contacts ( $2.749$  and  $2.732$  Å).

### 3.3. Cambridge Structural Database studies

One might wonder if the bent bond of the diazo group universally occurs. Thus, we searched the Cambridge Structural Database (CSD version 5.33 Nov. 2011) for diazo compounds, restraining our search to organic and noncoordinated compounds. As described in the experimental section, the search with restrictions, *i. e.*, no crystallographic disorder and an R-factor of less than 0.1, gave 150 (125 crystal structures) hits. For these 150 hits, the scatter plots of the C1-N1-N2 bond angle vs. the N1-N2 length are shown in Figure 3. Inspection of the C1-N1-N2 angle in Figure 3 indicates that the angles are mostly distributed in the range of  $177$ - $179^\circ$  and an angle of  $180^\circ$  is observed only in three structures.

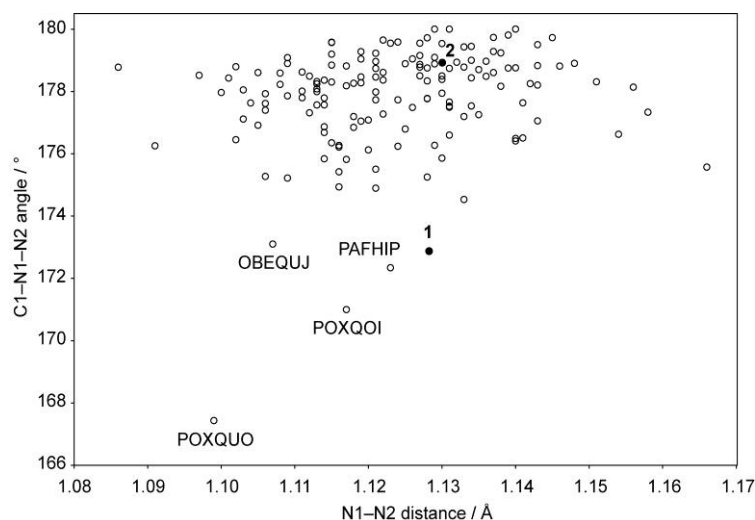
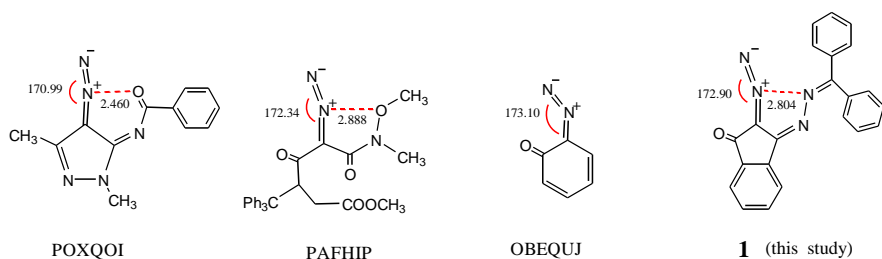


[Fig. 3. Scatter plot of CNN angle vs. N-N bond length of diazo functional group.]



[Scheme 2 Diazo compounds having highly bent CNN bond.]

As clearly shown in Fig. 3, **1** lies in the range of the most bent CNN bonds. We have extracted four entries with less than 174.0 Å, which are indicated by the CSD reference code (POXQUO [19], POXQOI [19], PAFHIP [20], OBEQUJ [21]) in Fig. 3. Their structures are shown in Scheme 2, along with that of **1**. Among those, the data of POXQUO appear to be removable because of their low reliability due to the small temperature factor of the nitrogen atom corresponding to the N1 atom as compared with those of other atoms. With respect to POXQOI, the result also seems to be suspicious because of the lack of hydrogen atom coordinates. In any event, the molecular structure of **1** definitely provides a new entry of bent diazo CNN bonds that are populated sparsely in CSD.

It should be determined which direction the  $C=N^+=N^-$  bond is bent to. Thus, we generated a scatter plot of the CNN angle vs. the twist angle of N2-N1-C1-R1. In this search, the following structures were excluded: (a) structures in which the difference between the N2-N1-C1-R1 and N2-N1-C1-R2 dihedral angles, accurately to be 180°, is less than 170°; (b) those with an N2-N1-C1 angle of 180°. With these filters, 143 structures were found, and for which the scatter plot of the C1-N1-N2 angle vs. the twist angle of N2-N1-C1-R1 is shown in Fig. 4. The dihedral angle is distributed in a wide range from 0 to 90°, although the number of entries gradually decreases with increasing dihedral angle. The most interesting feature is that the structure having a large bend angle of N2-N1-C1 angle adopts a small twist angle of N2-N1-C1-R1, that is, it bends in the plane made by N2, N1, C1, R1, and R2. Compound **1** and the four entries in the region less than 174° in Fig. 3 are found again in areas with low twist angles in Fig. 4.

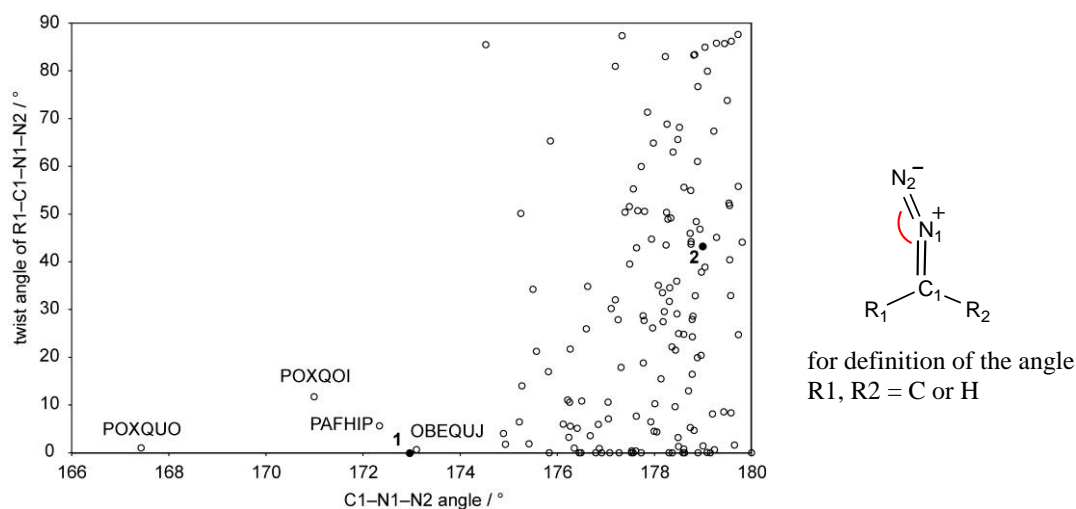


[Fig. 4. Scatter plot of the C1-N1-N2 angle vs. twist angle of N2-N1-C1-R1.]

In **1**, the intramolecular interaction between the spatially proximate nitrogen atom can be observed, as judged from the contact distance (2.804 Å), which is smaller than the sum of the van der Waals radius (1.55+1.55 Å). This is also true for POXQOI and PAFHIP. In these compounds, the CNN group is bent toward the opposite side of the interaction. The intramolecular heteroatom interaction with the N1 atom could be partially responsible for the bending of the C1-N1-N2 bond toward the back side of interaction.

As shown in Fig. 3 and Fig. 4, the C1-N1-N2 bonds are more or less bent rather than linear. Thus, the unsymmetrical structure observed in the CNN bond would be related to the R1-C1-N1 and R2-C1-N1 angles. Then, the distortion of the C1 carbon in the R1(C1N1N2)R2 framework was investigated using a scatter plot of the CNN angle vs. the difference between the R1-C1-N1 and R2-C1-N1 bond angles. Fig. 5 shows that such differences in the angles are mostly distributed in a region of less than 6°. However, with respect to the entries that have large bent CNN angles, the distortion is clearly pronounced compared with those of most other cases. **1** is also part of the group of highly deformed structures showing a difference of 8.08°. Thus, bending at the C1-N1-N2 bond should also be affected by the distortion of the R1-C1-N1 and R2-C1-N1 angles. This is supported by the DFT calculations, as described in the next section.

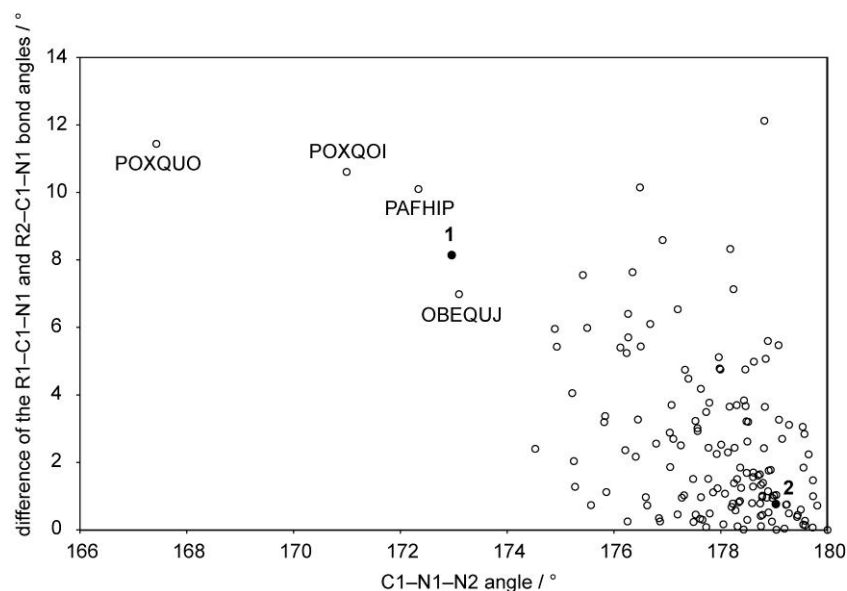


[**Fig. 5.** Scatter plot of CNN angle vs. difference between R1-C1-N1 and R2-C1-N1 bond angles.]

### 3.4. DFT calculations

To gain more insight into the bent structure of the diazo group, we carried out DFT calculations of various diazo compounds. First, to confirm the reliability of the computational method adopted in this study, we carried out calculations of diazo compounds, namely, those with a linear diazo group (DAZFUL11 and ENIGEO[22]), and an extremely bent diazo group (POXQUO) as well as for our diazo compounds **1** and **2**. For all these diazo compounds, crystallographic data are available. Selected parameters for their optimized geometries in comparison with those of the X-ray structure are shown along with the data obtained by X-ray crystal analyses for comparison in Table 3. We clearly observe from this table the good agreement between the experimental and calculated data for the diazo compounds, indicating the reliability of the DFT calculations adopted in this study. The N1-N2 bond in **1** and **2** is shorter than their N1-C1 bond, which suggests predominant participation of resonance structure B ( $>\text{C}^--\text{N}^+\equiv\text{N}$ ) and C ( $>\text{C}^--\text{N}=\text{N}^+$ ) in the structure of the diazo group. This was also supported by atomic-centered fitting charges to electrostatic potentials calculated by the Breneman's method [23]. The charges on C1, N1, and N2 are -0.421, 0.551, and -0.269, respectively for **1** and these for **2** are -0.347, 0.466, and -0.275, respectively.

[**Table 3** Selected geometrical parameters for diazo compounds **1**, **2**, POXQOI, DAZF11, and ENIGEO computed at 6-311++ G(d,p) level of theory and observed in X-ray crystallographic analysis. ]

As is evident from Table 3, the diazo group C1-N1-N2 in the symmetric molecular structure takes a linear geometry; hence, the N1 atom has an sp hybridization. It is therefore valid that the N1 atom takes basically a linear geometry, but suffers deformation due to steric and/or electronic interactions with neighboring substituents to deviate from the intrinsic position. We have also investigated the DFT optimized structures for eight model compounds (**3-10**) based on the cyclopentylidenecyclopentane framework. These compounds mimic a partial structure of POXQOI and are designed with the intention to induce steric hindrance to the diazo group by the substitution of the cyclopentylidene moiety, which is set close to the diazo group. The results of the DFT optimized structures are listed in Table 4, including difference in R1-C1-N1 and R2-C1-N1 bond angles, intramolecular distance between N1 and the atom (X) located most closely to N1 (X---N1), and distance made by subtraction of the van der Waals distance of X from X---N1 distance.

[**Table 4** Selected B3LYP/6-311++G(d,p) optimized geometries of cyclopentanylidene cyclopentanes, **3-10**.]

In all the compounds, the neighboring cyclopentylidene group permits the bending of the CNN bond toward the less hindered side, regardless of the existence of the carbonyl group at this side. Bending occurs in the plane made by cyclopentylidenecyclopentane and the diazo group. Furthermore, the substituents at the 2-position of the cyclopentylidene group (X=O, C, Br) enhance the bending of the C1-N1-N2 bond. We can see more clearly such steric effect from Fig. 6, which shows relationship between C1-N1-N2 bond angle and the value derived by subtraction of the van der Waals distance of X from the distance X---N1. The latter value was incorporated by taking into consideration that the atomic volume should more accurately reflect steric congestion than the X---N1 distance itself. Thus, on these DFT calculations, we could assume that the origin of the bend is principally the steric interaction.

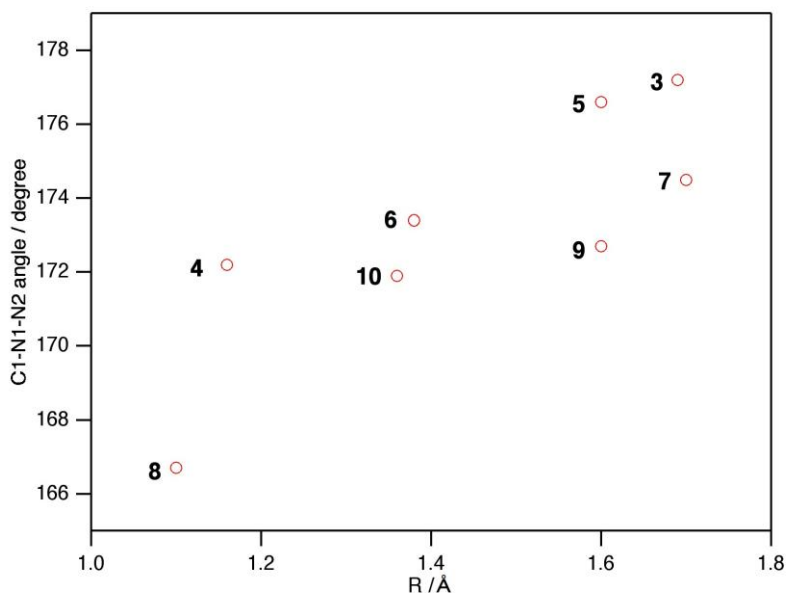


**[Fig. 6.** Relationship based on B3LYP/6-311++G(d,p) level calculations between C1-N1-N2 bond angle and the value resulting from subtraction of the van der Waals distance of X from the distance X----N1.]

Another interesting result is that the  $\alpha$ -keto diazocyclopentanes (**3**, **4**, and **5**) have a tendency to bend at a larger angle than the compounds without the  $\alpha$ -keto group (**7**, **8**, and **9**). Thus, it seems most likely that the carbonyl substituent on the opposite side of steric interaction in the model compounds exerts attractive interaction with the diazo CNN bond, resulting in the bending of the CNN group to this carbonyl side. As will be described later in this section, this assumption is supported by the potential surface calculations of 2-diazocyclopentanone.

As is depicted in Fig. 7, the theoretical calculations of eight model compounds also indicate a tendency of the C1-N1-N2 bond to bend more with increasing difference in the R1-C1-N1 and R2-C1-N1 bond angles, corresponding well to Fig. 5 obtained based by CSD retrieval.

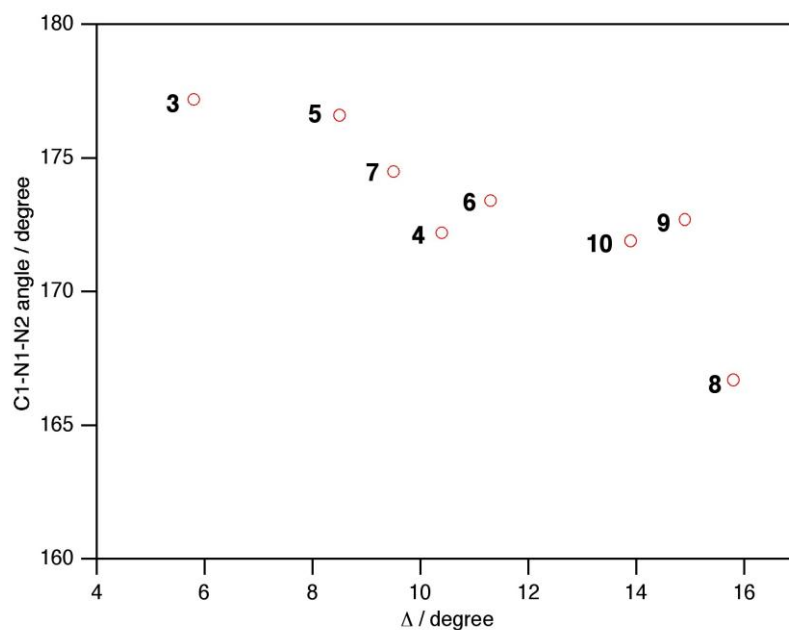
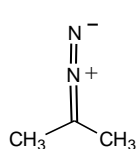
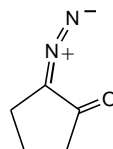


[**Fig. 7.** Relationship of C1-N1-N2 angle vs. difference in R1-C1-N1 and R2-C1-N1 bond angles calculated for eight model compounds (**3-10**).]

All the above results imply that the C1-N1-N2 and R1-C1-N1 angles are readily variable depending on the structural environment. Then, for a better understanding of the nature of these systems, the potential energy surfaces (PESs) according to the bend C1-N1-N2 angle were calculated for 2-diazopropane (**11**) and diazocyclopropanone (**12**) (Fig. 8). The optimized structure of **11** is symmetric, and its potential energies show a shallow minimum at a linear geometry of the C1-N1-N2 bond (Fig. 8-a). Upon the change in the C1-N1-N2 bond from 180° to 160°, the potential energy increases, but by only 4 kcal/mol.



**11**



**12**

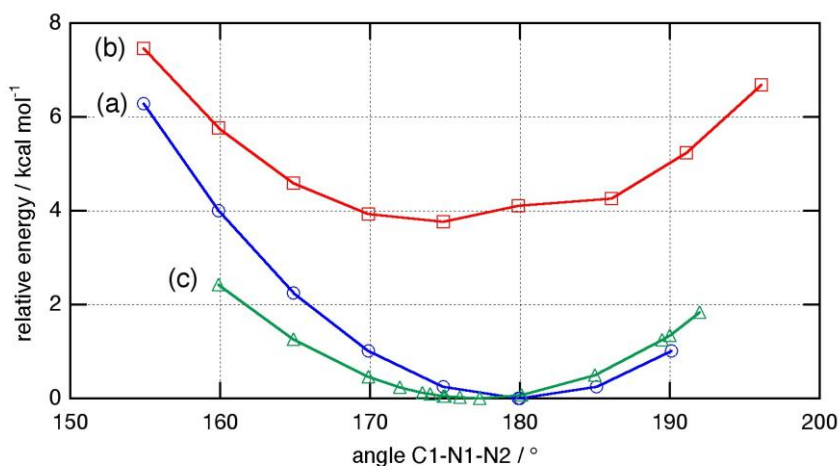
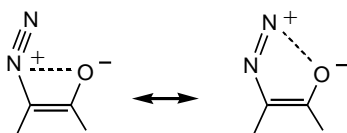


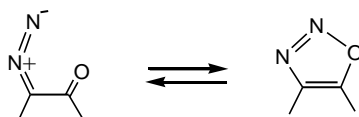
[**Fig. 8.** Potential energy surfaces along path of bending C1-N1-N2 angle, for (a) **11** with equal angles of R1-C1-N1 and R2-C1-N1, (b) **11** with angles of R1-C1-N1=130° and R2-C1-N1= 120°, and (c) **12**.]

The PES was also investigated for a distorted structure of **11**, in which the R1-C1-N1 angle is fixed at 130° and the R2-C1-N1 is at 120°. Under such distortion, the potential surfaces for bending CNN are shifted higher in energy and a potential minimum appears at 172° on the R2-C1-N1 side (Fig. 8-b). The energy surface comes out more shallow as compared with that in the case of a symmetrical structure, indicating that the bent R1-C1-N1 bond facilitates further bending of the diazo C1-N1-N2 bond. Only 2 kcal/mol is required to bend the C1-N1-N2 bond to 160°.

The PES for 2-diazocyclopentanone (Fig. 8-c) resembles that for the distorted 2-diazopropane. A single minimum shifts to the  $\alpha$ -carbonyl side at 176° with a shallow profile: only 1.2 kcal/mol is required to bend the CNN bond from 176° to 160°. These results are consistent with the finding from Table 6 and support the idea that the carbonyl group at the  $\alpha$ -position exerts attractive electronic effects to facilitate the bending of the diazo group. An experimental result supporting this idea is provided by the X-ray crystal analysis of  $\alpha$ -diazocyclohexanone, OBEQUIJU, referred to as a highly bent example; its CNN bond is bent to the carbonyl side despite the absence of a sterically congested group on the other side.



The most plausible interaction between the carbonyl and diazo groups is assumed to be the electrostatic interaction depicted in Scheme 3. Some  $\alpha$ -keto diazoalkanes undergo valence isomerization to oxadiazole [24]. In this isomerization, the involvement of an extremely bent diazo group is predictable according to the results of our present investigation.



#### 4. Conclusion

The isolation of a novel diazo compound 2-diazo-3-diphenylmethylenehydrazono-2-indanone (**1**) prompted us to search the CSD for diazo compounds, because the  $C=N^+=N^-$  bond of **1** was bent by  $172.9^\circ$  in contrast to the common understanding that the  $C=N^+=N^-$  bond takes a linear geometry with an N1 atom of sp hybridization. The CSD search disclosed that extensive examples of bent C1-N1-N2 bonds exist contrary to our presumption and that  $172.9^\circ$  is one of the most bent C1-N1-N2 entries. It was revealed that diazo compounds with bent bonds tend to increase their R1-C1-N1 angles. The DFT calculations based on the 6-311++G(d,p) level indicated that the bending of the diazo C1-N1-N2 bond is principally ascribable to steric congestion. When the carbonyl group is substituted at the  $\alpha$ -position of the C1-N1-N2 group, the carbonyl group exerts an attractive interaction to bend the C1-N1-N2 bond towards this side. For **1**, both factors deduced in this investigation are involved in bringing about a large bending angle to the C1-N1-N2 bond.

#### Acknowledgements

This work was partially supported by a Grant-in-Aid for Scientific Research (no. 21550048) from the Ministry of Education, Culture, Sports, Science and Technology, Japan.

## References

- [1] (a) S. Patai, Ed., *The Chemistry of Diazonium and Diazo Groups*, Wiley, New York, 1978.  
(b) M. Regitz, G. Mass, *Diazo Compounds. Preparation and Syntheses*, Academic Press, Orland, 1986.  
(c) H. Zollinger, *Diazo Chemistry*, VCH, Weinheim, Vol. 1, 1994; Vol. 2, 1995.
- [2] (a) R. A. Moss, M. S. Platz, M. Jones, Jr., Ed., *Reactive Intermediate Chemistry*, Wiley-Interscience, Hoboken, 2004.  
(b) U. H. Brinker, Ed., *Advances in Carbene Chemistry*, Vol. 3, Elsevier, Amsterdam, 2001.
- [3] K. Clusius and U. Luthi, *Helv. Chim. Acta* 40 (1957) 445.
- [4] In ref 1b: Chapter 1: pp10-23
- [5] SIR92: A. Altomare, G. Cascarano, C. Giacovazzo, A. Guagliardi, M. Buria, G. Polidori, M. Camalli, *J. Appl. Crystallogr.* 27 (1994) 435.
- [6] *CrystalStructure 3.8: Crystal Structure Analysis Package*; Rigaku and Rigaku/MS (2000-2006): The Woodlands, TX.
- [7] *CRYSTALS Issue 11*: J. R. Carruthers, J. S. Rollett, P. W. Betteridge, D. Kinna, L. Pearce, A. Larsen, E. Gabe, *Chemical Crystallography Laboratory*: Oxford, UK, 1999.
- [8] F. H. Allen, *Acta Crystallogr. Sect. B: Struct. Sci.* B58 (2002) 380.
- [9] *Con Quest*: F. H. Allen, O. Kennard, *Chem. Des. Autom. News* 8 (1) (1993) 31.
- [10] M.J. Frisch, G.W. Trucks, H.B. Schlegel, G.E. Scuseria, M.A. Robb, J.R. Cheeseman, G. Scalmani, V. Barone, B. Mennucci, G.A. Petersson, H. Nakatsuji, M. Caricato, X. Li, H.P. Hratchian, A.F. Izmaylov, J. Bloino, G. Zheng, J.L. Sonnenberg, M. Hada, M. Ehara, K. Toyota, R. Fukuda, J. Hasegawa, M. Ishida, T. Nakajima, Y. Honda, O. Kitao, H. Nakai, T. Vreven, J.A. Montgomery, Jr., J.E. Peralta, F. Ogliaro, M. Bearpark, J.J. Heyd, E. Brothers, K.N. Kudin, V.N. Staroverov, R. Kobayashi, J. Normand, K. Raghavachari, A. Rendell, J.C. Burant, S.S. Iyengar, J. Tomasi, M. Cossi, N. Rega, J.M. Millam, M. Klene, J.E. Knox, J.B. Cross, V. Bakken, C. Adamo, J. Jaramillo, R. Gomperts, R.E. Stratmann, O. Yazyev, A.J. Austin, R. Cammi, C. Pomelli, J.W. Ochterski, R.L. Martin, K. Morokuma, V.G. Zakrzewski, G.A. Voth, P. Salvador, J.J. Dannenberg, S. Dapprich, A.D. Daniels, O. Farkas, J.B. Foresman, J.V. Ortiz, J. Cioslowski, D.J. Fox, *Gaussian 09, Revision A.02*, Gaussian, Inc., Wallingford CT, 2009.
- [11] A.D. Becke, *J. Chem. Phys.* 98 (1993) 5648.

- [12] A.D. Becke, J. Chem. Phys. 107 (1997) 8554.
- [13] C. Lee, W. Yang, G.R. Parr, Phys. Rev. B, 37 (1988) 785.
- [14] M. B. Rubin, R. Gleiter, Chem. Rev. 100 (2000) 1121.
- [15] (a) J. Jayashankaran, R. Durga, R. S. Manian, M.R. Sivaguru, R. Raghunathan, Tetrahedron Lett. 47 (2006) 5535.
- (b) J. Jayashankaran, R. D. R. S. Manian, R. Raghunathan, Synthesis (2006) 1028.
- (c) M. S. Leonard, D. B. Hauze, P. J. Carroll, M. M. Joullie, Tetrahedron 59 (2003) 6933.
- (d) M. F. Aly, H. Ardill, R. Grigg, S. Leong-Ling, S. Rajviroongit, S. Surendrakumar, Tetrahedron Lett. 28 (1987) 6077.
- (e) H. Ardill, R. Grigg, V. Sridharan, S. Surendrakumar, S. Thianpetanagul, S. J. Kanajun, Chem. Soc. Chem. Commun. (1986) 602.
- (f) R. Grigg, J. F. Malone, T. Mongkolaussavaratane, S. Thianpatanagul, J. Chem. Soc. Chem. Commun. (1986) 421.
- (g) P. A. Crooks, Chem. and Industry (1980) 467.
- (h) A. Schönberg, E. Singer, B. Eschenhof, G-A. Hoyer, Chem. Berichte (1978) 3058.
- (i) M. Israel, L. C. Jones, E. J. Modest, J. Heterocyclic. Chem. (1972) 255.
- (j) R. H. F. Manske, Q. A. Ahmed, Canad. J. Chem. 48 (1970) 1280.
- (k) R. Shapibo, N. Chatterjie, J. Org. Chem. 35 (1970) 447.
- [16] M. Regitz and G Heck, Chem. Ber. 97 (1964) 1482.
- [17] in Ref 1b: Chapter 9: pp 257-292.
- [18] Z. Wang, Comprehensive Organic Name Reactions and Reagents, Wiley-Interscience, Hoboken, 2009.
- [19] G. Daidone, M. L. Bajardi, S. Plescia, D. Raffa, D. Schillaci, B. Maggio, F. Benetollo, G. Bombieri, Eur. J. Med. Chem. 31 (1996) 461.
- [20] Y. S. M. Vaske, M. E. Mahoney, J. P. Konopelski, D. L. Logow, W. J. McDonald, J. Am. Chem. Soc. 132 (2010) 11379.
- [21] M. Kawano, K. Hirai, H. Tomioka, Y. Ohashi, J. Am. Chem. Soc. 129 (2007) 2383.
- [22] P. J. Davis, L. Harris, A. Karim, A. L. Thompson, M. Gilpin, M. G. Moloney, M. J. Pound, C. Thompson, Tetrahedron Lett. 52 (2011) 1553.
- [23] C. M. Breneman, K. B. Wiberg, J. Comp. Chem. 11 (1990) 361.
- [24] R. Schulz, A. Schweig, Angew. Chem., Int. Ed. Engl. 18 (1979) 692.

**Table1** Crystal and experimental data of 1 and 2

		1	2
Chemical		C <sub>22</sub> H <sub>14</sub> ON <sub>4</sub>	C <sub>35</sub> H <sub>24</sub> N <sub>6</sub>
Formula			
Formula Weight		350.38	528.61
Crystal Color,		yellow needle	yellow platelet
Habit			
Crystal size		0.30 x 0.30 x 0.05	0.95 x 0.10 x 0.05
Crystal System		monoclinic	monoclinic
Space Group		<i>P</i> 2 <sub>1</sub> / <i>a</i> (#14)	<i>P</i> 2 <sub>1</sub> / <i>c</i> (#14)
Lattice		<i>a</i> = 7.5248(19)	<i>a</i> = 12.586(5) Å
Parameters		Å	<i>b</i> = 10.896(4) Å
		<i>b</i> = 20.239(6) Å	<i>c</i> = 20.377(8) Å
		<i>c</i> = 11.665(3) Å	<i>β</i> = 102.611(16)°
		<i>β</i> = 105.621(10)°	<i>V</i> = 2726.9(18)
		<i>V</i> = 1710.9(8)	Å <sup>3</sup>
		Å <sup>3</sup>	
Z value		4	4
<i>D</i> <sub>calc</sub>		1.360 g/cm <sup>3</sup>	1.287 g/cm <sup>3</sup>
F <sub>000</sub>		728.00	1104.00
Radiation		MoKα (λ = 0.71075 Å)	MoKα (λ = 0.71075 Å)
μ(MoKα)		0.871 cm <sup>-1</sup>	0.785 cm <sup>-1</sup>
2θ <sub>max</sub> cutoff		55.0°	55.0°
No. of reflections		17512	26086
collected			
No. of		3911	6228
independent			
reflections			
Residuals: R1		0.036	0.048
( <i>I</i> > 2.00σ( <i>I</i> ))			
Residuals: wR2		0.063	0.042
( <i>I</i> > 2.00σ( <i>I</i> ))			
Goodness of Fit		1.03	0.95
Indicator			
Maximum peak		0.23 e <sup>-</sup> /Å <sup>3</sup>	0.50 e <sup>-</sup> /Å <sup>3</sup>
in Final Diff. Map			

Minimum peak in Final Diff. Map	-0.19 e <sup>-</sup> / Å <sup>3</sup>	-0.48 e <sup>-</sup> / Å <sup>3</sup>
Measurement	Rigaku RAXIS-RAPID	Rigaku RAXIS-RAPID
Program System	RigakuCrystalStructure 3.8.2	RigakuCrystalStructure 3.8.2
Structure determination	direct methods (SHELX 97)	direct methods (SIL92)
Refinement	full-matrix least-squares on $F^2$	full-matrix least-squares on $F^2$
CCDC deposition number	CCDC885009	CCDC885010

---

**Table 2** Selected bond lengths (Å) and angles (°) for **1** and **2**

	<b>1</b>	<b>2</b>
N1-N2	1.128(2)	1.130(3)
N1-C1	1.319(2)	1.320(3)
C1-C2	1.467(2)	1.463(3)
C1-C9	1.4451(19)	1.445(3)
O1-C2	1.2204(17)	
N3-C9	1.2885(18)	
N3-N4	1.3964(17)	1.409(3)
N5-N6		1.402 (2)
N2-N1-C1	172.89(14)	179.0(2)
N1-C1-C2	120.19(12)	123.9(2)
N1-C1-C9	128.27 (14)	124.7(2)
O1-C2-C1	127.42(14)	

**Table 3** Selected geometrical parameters for diazo compounds **1**, **2**, POXQOI, DAZF11, and ENIGEO computed at 6-311++ G(d,p) level of theory and observed in X-ray crystallographic analysis.

Compd.		N1-N2 / Å	N1-C1 / Å	C1-N1-N2 / °	R1-C1-N1 / °	R1-C1-N1 / °
<b>1</b>	Calc.	1.126	1.309	172.3	120.5	128.7
	Cryst.	1.128	1.319	172.9	120.19	128.17
<b>2</b>	Calc	1.126	1.315	180	125.2	125.2
	Cryst	1.130	1.320	179.0	123.9	124.7
<b>POXQOI</b>	Calc	1.122	1.324	168.4	121.8	131.3
	Cryst	1.117	1.3169	171	120.8	131.4
<b>DAZF11</b>	Calc	1.137	1.301	180	125.5	125.5
	Cryst	1.134	1.317	179.44	125.47	
		1.133	1.322	179.43	125.02	125.3
<b>ENIGEO</b>	Calc	1.139	1.309	180	116.8	116.8
	Cryst	1.146	1.313	178.81	117.3 116.8	114.9

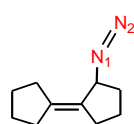
**Table 4** Selected B3LYP/6-31++G(d,p) optimized geometries of cyclopentanylidene-cyclopentanes, **3-10**.

$\Delta$ : difference between R1-C1-N1 and R2-C1-N1 bond angles.

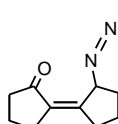
X---N1: intramolecular distance between N1 and X, the atom located most closely to N1.

R: distance derived by subtraction of the van der Waals distance of X from X---N1 distance.

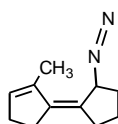
	N1-N2/Å	C1-N1/Å	C1-N1-N2	R1-C1-N1	R2-C1-N1	$\Delta$	X---N1	R
<b>3</b>	1.145	1.294	177.2	126.6	120.8	5.8	2.776	1.69
<b>4</b>	1.131	1.312	172.2	128.4	118.0	10.4	2.684	1.16
<b>5</b>	1.144	1.295	176.6	127.2	118.7	8.5	2.692	1.60
<b>6</b>	1.129	1.310	173.4	128.8	117.5	11.3	3.083	1.38
<b>7</b>	1.131	1.308	174.5	128.2	118.7	9.5	2.785	1.70
<b>8</b>	1.121	1.326	166.7	131.2	115.4	15.8	2.621	1.10
<b>9</b>	1.131	1.307	172.7	130.8	115.9	14.9	2.686	1.60
<b>10</b>	1.128	1.311	171.9	130.1	116.2	13.9	3.206	1.36



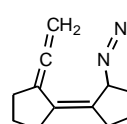
**3**



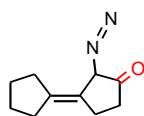
**4**



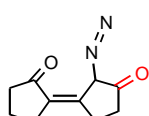
**5**



**6**



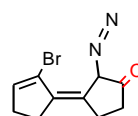
**7**



**8**



**9**



**10**